ACS SENSORS

pubs.acs.org/acssensors

Perspective

Overtone Spectroscopy for Sensing—Recent Advances and Perspectives

Alina Karabchevsky,* Uzziel Sheintop, and Aviad Katiyi

Cite This: https://doi.org/10.1021/acssensors.2c00655

Read Online

ACCESS | Metrics & More | Article Recommendations

ABSTRACT: In this perspective, we report an opinion on overtone spectroscopy for sensing and discuss the nature of the opportunities perceived for specialists. New spectroscopic strategies can potentially be extended to detect other common toxic byproducts in a chip-scale label-free manner and to enhance the functionality of chemical and biological monitoring. Nevertheless, the full potential of overtone spectroscopy is not yet exhausted, challenges must be overcome, and new avenues await. Within this Perspective, we look at where the field currently stands, highlight several successful examples of overtone spectroscopy based sensors and detectors, and ask what it will take to advance current state-of-the-art technology. It is our intention to point out some potential blind spots and to inspire further developments.

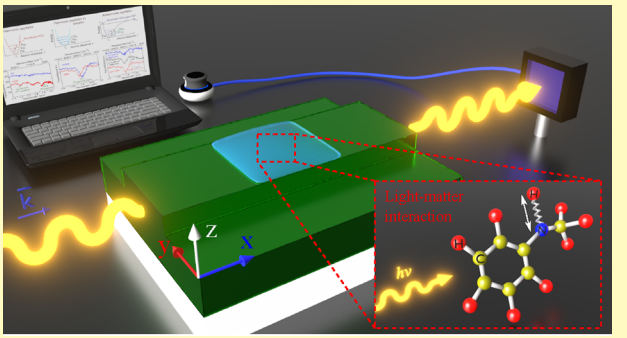

KEYWORDS: *molecular overtones, optical waveguide, near-infrared spectroscopy, integrated photonics, sensing*

Fingerprints provide a reliable means of identification. That is the essential explanation for why fingerprints have replaced other methods of identification. Ancient artifacts with carvings similar to friction ridge skin have been discovered in many places throughout the world. Prehistoric picture writing of a hand with ridge patterns was discovered on a cliff in Nova Scotia. In ancient Babylon, fingerprints were used on clay tablets for business transactions. The attribution of fingerprints as chemical elements began with the work of German physicists Robert Bunsen and Gustav Kirchhoff.[1] Their spectrum-observation apparatus is shown in Figure 1.

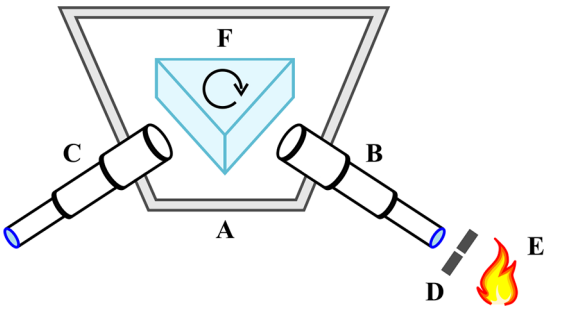

Figure 1. Spectrum-observation apparatus of Bunsen and Kirchhoff. The two inclined sides of the box **A**, which are placed at an angle of about 58° from each other, carry the two small telescopes **B** and **C**. The ocular lenses of the first telescope are removed, and in their place is inserted a plate, in which a slit **D** made by two brass knife-edges is so arranged that it coincides with the focus of the object-glass. The glass-lamp **E** stands before the slit in a position such that the mantle of the flame is in a straight line with the axis of the telescope **B**. A hollow prism **F** filled with bisulfide of carbon with a refracting angle of 60° is placed between the telescopes. By rotating the prism, each different line of the spectrum emitted from the gas lamp will move to the output telescope (**C**).

WHAT ARE THE CHALLENGES IN OVERTONE SPECTROSCOPY?

Spectroscopy focuses on the interaction between radiation and matter[2] and can be used for remote and on-site detection. The energy of a molecule can be divided to electronic, vibrational, rotational, and translational energy. When illuminated with infrared (IR) radiation, the atoms in the molecule start to vibrate. Each atom can vibrate in different modes, resulting in distinct absorption bands for different atoms that give information about the molecular structure. Vibration spectroscopy is based on detection of the absorption of photons that cause an atom's bond in the molecule to vibrate. Each molecule can have a different number of vibrational modes with different excitation energy. Each vibrational mode has a probability to occur. The rate of transitions can be defined by Einstein coefficient as[3]

Received: March 28, 2022
Accepted: August 29, 2022

$$B = \frac{|\boldsymbol{\mu}_{ij}|^2}{6\varepsilon_0 \hbar^2} \quad (1)$$

where ε_0 is the permittivity of free space, $\hbar$ is the reduced Planck constant, and $\boldsymbol{\mu}_{ij}$ is the electric dipole transition moment from state i to state j which is defined as

$$\boldsymbol{\mu}_{ij} = \left\langle i|\boldsymbol{\mu}|j \right\rangle = \int \psi_i^* \boldsymbol{\mu} \psi_j \, \mathrm{d}r \quad (2)$$

where ψ is the wave function for the state (i or j) and $\boldsymbol{\mu}$ is the electric dipole moment, defined as

$$\boldsymbol{\mu} = \boldsymbol{\mu}_0 + \sum_i \left(\frac{\partial \boldsymbol{\mu}}{\partial Q_i}\right)_0 Q_i + \frac{1}{2}\sum_{i,j}\left(\frac{\partial^2 \boldsymbol{\mu}}{\partial Q_i \partial Q_j}\right)_0 Q_i Q_j + \ldots \quad (3)$$

where $\boldsymbol{\mu}_0$ is the equilibrium value of the dipole moment, 0 is the value at equilibrium, and Q is the linear combination of the displacements.

The transition dipole moment is nonzero only when there is a change in the dipole moment during the vibration. Therefore, the selection rule for IR absorption is that a photon can be absorbed only when a change in the dipole moment occurs during the vibration.

Initially, the first assumption was that the molecule behaves like a harmonic oscillator and only absorption by fundamental vibrations can occur. Later it was found that the molecules have electrical and mechanical anharmonicity that causes the molecules to behave as an anharmonic oscillator. An estimated model for an anharmonic oscillator is the Morse potential function as shown in Figure 2. The Morse potential function,

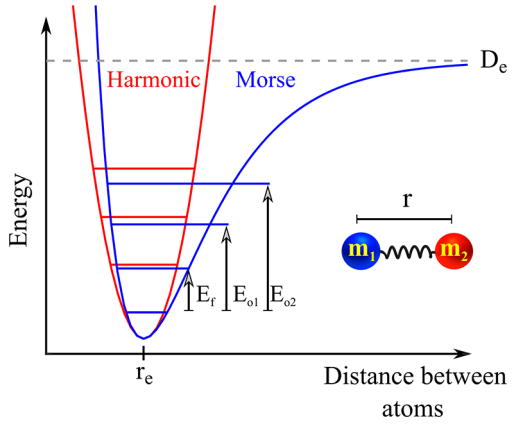

Figure 2. Illustration of the Morse potential function for anharmonic vibration compared to the potential function for harmonic vibration. E_f - fundamental vibrational transition energy. E_{oi} is the i^{th} overtone vibrational transition energy. D_e is the dissociation energy.

in contrast to the harmonic model, includes the effect of bond breaking D_e and the anharmonicity of the bonds. Due to the mechanical and electrical anharmonicities of the molecule, the higher-order derivatives in the dipole moment in eq 3 are nonzero and, therefore, cannot be neglected. Due to the anharmonicity, the probability of transitions of $\Delta v > 1$ (for example $0 \rightarrow 2$, $0 \rightarrow 3$, and $0 \rightarrow 4$) is nonzero and the transitions are allowed. The transition of $\Delta v > 1$ is called overtone. Vibrational overtones occur in the near-IR (780–2500 nm or 14 000 to 4000 cm^{-1}). However, the absorption of overtone is an order of magnitude lower as compared to the fundamental vibrations (and between adjacent overtone levels such as between the first overtone ($0 \rightarrow 2$) and second overtone ($0 \rightarrow 3$)) which makes vibration overtone spectroscopy very challenging.

WHAT ARE THE BARRIERS THAT SENSING CONFIGURATIONS FACE?

The Indicator: Are We Innovating in the Right Direction? Overtone spectroscopy can be implemented in a variety of methods. The most common absorption spectroscopy configuration to date is free-space spectroscopy. The optical path in which the light-matter interaction takes place in a bulk medium and involves free-space coupling between the light source and the sensor. However, the sensitivity of free-space systems relays on the optical path which in many cases needs to be very long (from cm to hundreds of meters). There are a few methods for increasing the sensitivity while reducing the path-length of spectroscopic devices such as multipass systems, and fiber-coupled sources. Yet these approaches consist of discrete optical components, did not extract the full potential of miniaturization, and did not succeed in obtaining an integrated form of the sensor with on-chip CMOS compatibility. Another drawback of the free-space spectroscopy systems linked to the use of bulk optics is the need for system alignment and the effect on the system stability, due to the sensitivity to the influence of temperature changes and vibrations.

An ideal alternative approach to free-space absorption spectroscopy is a photonic integrated circuit (PIC).[4] It enables chip-scale spectroscopy in a miniaturized, robust, stable, and affordable platform with low power consumption. This method is becoming more and more mature, and enormous progress has been shown for all the building blocks needed for such a type of spectroscopy, for example, light sources, including coherent and narrowband sources,[5−8] waveguides,[9] and sensors,[10,11] as well as components used to manipulate the light, such as modulators,[12] polarizers, switches,[13,14] couplers,[7] beam splitters,[15] and filters.[10,16,17] The sensing using the PIC platform can also utilize designs like metamaterials[17] and phenomena like solitons.

The principle of absorption spectroscopy is based on the Beer–Lambert law:[18] the transmitted intensity I, while neglecting the coupling losses, is given by $I = I_0 \exp(-\Gamma\alpha L)$, where I_0 is the incident intensity, α is the absorption coefficient of the medium, L is the interaction length, and Γ is the medium-specific absorption factor determined by dispersion enhanced light-matter interaction. In conventional free-space systems, $\Gamma = 1$; therefore, L must be large to achieve a suitable sensitivity of measured I/I_0. Using perturbation theory one can show that $\Gamma = f \times \frac{c/n}{v_g}$[19] where c is the velocity of light in vacuum, v_g the group velocity in a medium of effective index n, and f is the filling factor denoting to the relative fraction of the electric field residing in the analyte. It shows that small group velocity, v_g, significantly enhances the absorption. Furthermore, the greater the electric field overlaps with the analyte, the greater the effective absorption by the medium becomes.[20] PICs are a good platform to fulfill both conditions of low v_g and high f in many design approaches.

To increase the light–analyte interaction, one can increase the overlap of the optical mode of the waveguide and an analyte under investigation. For this, some means need to be developed to increase the penetration depth of the evanescent

https://doi.org/10.1021/acssensors.2c00655
ACS Sens. XXXX, XXX, XXX−XXX

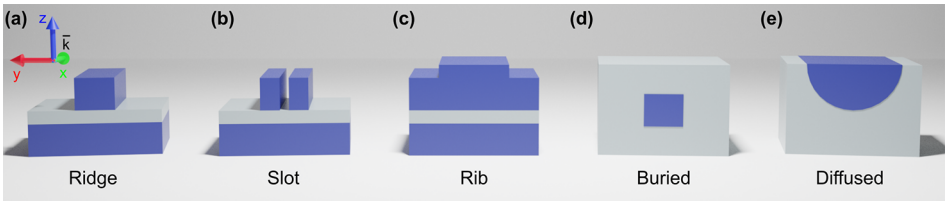

Figure 3. Cross-section of common optical waveguide configurations: (a) ridge waveguide, (b) slot waveguide, (c) rib waveguide, (d) buried waveguide, and (e) diffused waveguide.

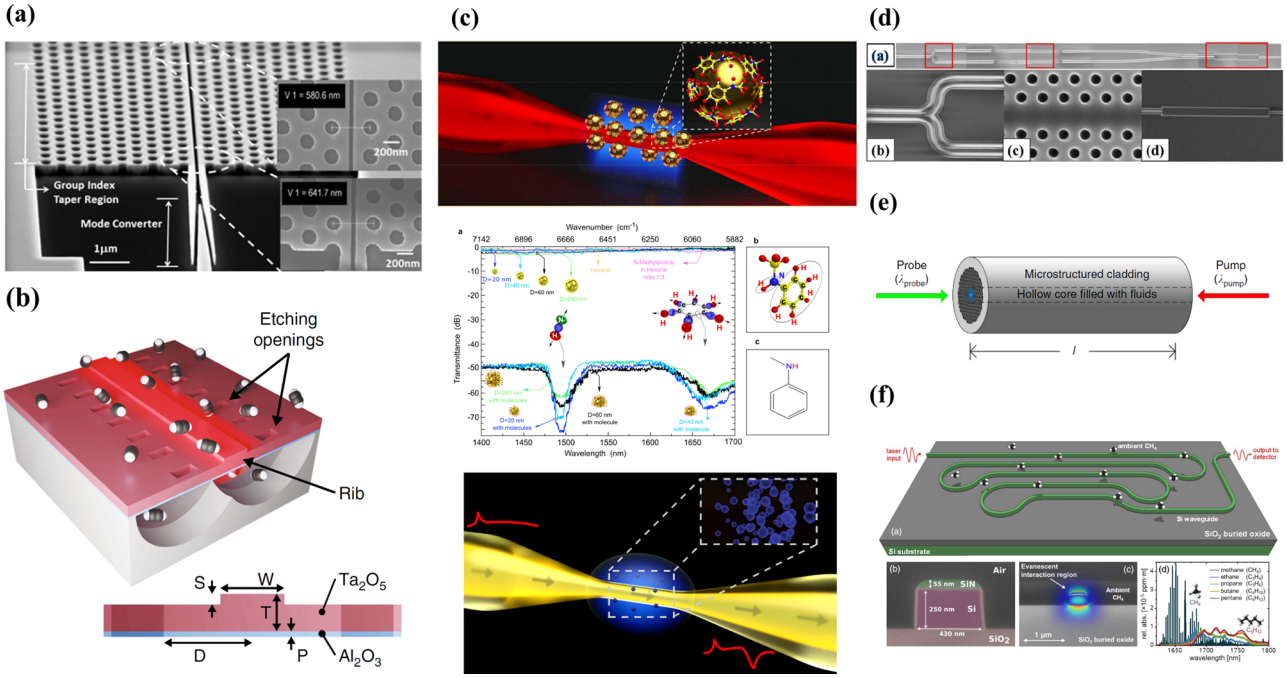

Figure 4. On chip waveguide architecture for absorption spectroscopy. (a) Scanning electron microscopy (SEM) image of the fabricated PC slot waveguide device (reprinted with permission from ref 20, copyright 2011 AIP Publishing). (b) Schematics of the free-standing shallow rib waveguide interacting with molecules (reprinted with permission from ref 31, copyright 2021 Nature). (c) (top) Illustration of the tapered fiber with gold nanoparticles surface modification followed by the measured transmission spectrum (reprinted with permission from ref 32, copyright 2018 ACS Publications) and (bottom) tapered fiber for monitoring cancer treatment efficiency (reprinted with permission from ref 33, copyright 2020 Elsevier). (d) Scanning electron microscopy (SEM) images of a photonic crystal waveguide for the detection of xylene and trichloroethylene in water (reprinted with permission from ref 34, copyright 2013 OSA). (e) Illustration of a hollow core fiber for gas detection (reprinted with permission from ref 35, copyright 2015 Nature). (f) Silicon photonic waveguide absorption spectrometer (SPWAS) for CH_4 with zigzag configuration (reprinted with permission from ref 36, copyright 2017 OSA).

field with the benefit of slow group velocity, v_g, as we will discuss further.

As mentioned above, optical waveguides are becoming an attractive building block in a variety of systems due to their unique features such as large evanescent field, compactness, and mostly, the ability to be configured to the required application.[4] Waveguides used in integrated photonics are planar and composed of at least three layers: the substrate, the guiding layer (or core), and a cladding (air or others). The light is guided in the waveguide due to total internal reflection (TIR).[21] Common configurations of waveguides[22] include slab, strip loaded, ridge, rib, buried, and diffused, as shown in Figure 3. Each configuration has properties that can be utilized for different applications. For example, a ridge waveguide can be used for sensing due to the large evanescent field, while a buried waveguide configuration can be used for optics communication. Optical waveguides can be used for both passive and active applications such as splitters,[23,24] directional couplers,[25,26] optical modulators,[27,28] and light sources.[29,30]

Optical waveguides can also be used for overtones spectroscopy. The following waveguide architectures have perspective in improving the free-space spectroscopy via efficient on-chip light propagation:

Slot Waveguides. In a slot waveguide, a narrow air slot is introduced into a ridge waveguide, or equivalently there are two closely spaced waveguides, as shown in Figure 4a. The air separation is on a scale within the decay length of the evanescent field from each of the two adjacent waveguides. The two evanescent tails can superpose and get enhanced within the narrow air region separating them. This combination can form a mode of propagation in which most of the light intensity is contained within the low refractive index region, even though total internal reflection is used for guidance. As a result, in a slot waveguide, the interaction between the optical field and the analyte can be very high, as the majority of the mode overlaps with the analyte, rather than just the tail as in the waveguide designs with no slots in them.[37] This may lead to the enhanced light−matter interaction, which

https://doi.org/10.1021/acssensors.2c00655
ACS Sens. XXXX, XXX, XXX−XXX

Table 1. Common Materials and Architectures for On-Chip Overtone Spectroscopy in Near-Infrared

material	waveguide design	analyte-LoD	$\lambda - \Gamma$ (EFR)	details	ref
silicon	TM ridge	CH_4 - 100 ppm	1651 nm-0.255	100 mm path length with snake-like design (16 mm^2 footprint)	36
silicon	microring resonator	NMA (N−H) -<2 nL	1483 nm	100 μm radius with Q > 100 000 with 1 nm resolution and effective free-space path lengths up to 5 mm	41
chalcogenide	ridge	NMA (N−H) - 0.7 vol %	1496 nm	$Ge_{23}Sb_7S_{70}$ glass films onto oxide coated silicon wafers; a Y-splitter with 1 arm as reference	40
silicon	PC slot	CH_4 - 100 ppm	1665 nm	300 μm long, 90 nm wide slot, n_g = 30−100 (40 at 1665 nm)	48
silicon	PC	xylene (C−H) - 1 ppb (v/v), TCE (C−H) - 10 ppb (v/v)	1674 nm, 1644 nm	n_g = 23 at 1644 nm - 33 at 1674 nm, in water	34
silicon	PC slot	xylene (C−H) - 100 ppb (v/v)	1665 nm	300 μm long, 75 nm wide slot, n_g = 20 - in water	20
GaInP	PC slab	C_2H_2	1534 nm - 0.31(TE), 1(TM)	1.5 mm long, n_g = 1.5 (TM), 6.7(TE)	49
silica (clad)	antiresonant HC fiber	CH_4 - 24 ppb, CO_2 - 144 ppm	1574 nm	a diameter of 84 μm. within 1 m path length	52
silicon	SWG	CH_4 - 1.42 ppm	1651 nm -1.1	14.4 mm long, n_g = 5.6	45
silicon	spiral-shaped rib	glucose (C−H) - 1 mM	1590 nm		56
chalcogenide	ridge	PEA (N−H) - 0.1 mol L^{-1}	1550 nm -0.05−0.15	10 mm long, $Ge_{25}Sb_{10}Se_{65}$	57

can in some circumstances reach 10 times better than conventional rectangular waveguides,[38] and can be used for on-chip spectroscopy in mid-IR but also for the overtone spectroscopy in near-infrared.[20]

Suspended Waveguides. For also utilizing the part of the evanescent field that travels below the core for the light−matter interaction, a suspended design can be introduced, as shown in Figure 4b. In a suspended design, the waveguide is elevated and part of the substrate is exposed to the analyte. It left the bottom section of the waveguide bare, so the increased portion of the field is taking part in the interaction with the analyte as in refs 31 and 39. It is worth noting that in suspended waveguides, the electric field intensity distribution of a transverse magnetic *TM mode* is characterized by a larger portion of the field which propagates beyond the waveguide core, as compared to a transverse electric (TE) mode which is more confined in the core. Therefore, the TM mode can be utilized for an enhanced light-matter interaction on-chip spectroscopy like in ref 40. Also, several waveguide architectures can be integrated on a chip such as a microring resonator,[41] zigzag design,[36] and suspended waveguide[31] to demonstrate the TM-mode based sensing capabilities.

Tapered Waveguides. One of the methods that can be used to enhance the sensitivity is by decreasing the confinement of the mode in guided wave structure. By minimizing the dimensions of the guiding medium, the confinement of the mode decreases. As a result, the fraction of the power and the penetration depth of the evanescent field increases. Tapered fiber can be used for biological[33] and chemical[32] detection. This sensing method is based on the evanescent field absorption. Along the propagation, a fraction of the field in a guided mode can penetrate beyond the guiding layer and exponentially decay. This fraction of the field is called the evanescent field. Guided wave structures can be used for an evanescent field sensor, which is also named the "attenuated total reflection" (ATR) sensor. It is based on the interaction between the evanescent field and the analyte. It requires little or no sample preparation. In addition, ATR is good for highly absorptive samples[42] due to the small penetration depth of the evanescent field. Also ring-resonators can be used as an evanescent field sensor.[43] It exhibits enhanced sensitivity due to the strong influence of the resonator environment. It can sense temperature, refractive index, and even strain. The resolution of the sensor is defined by the wavelength distance between two resonances (FSR, free spectral range). Using a microring resonator, the spectra of *N*-methylaniline (NMA) from 1.46 to 1.6 μm can be identified with a resolution of 1 nm.[41] However, it cannot provide broadband sensing, due to limitations of the FSR-based method.[41] Another option is the use of glass waveguides. Glass waveguides can be used for molecular overtones in near-infrared while integrated with a microfluidic chip. In addition, diffused waveguides were used to detect N−H bond overtone absorption around 1.5 μm.[44] The waveguides were pretreated by negative charge using plasma oxygen, which is not suitable for on-site long-time measurements. Recently, optical waveguides were proposed for detecting gas. The slow light phenomenon in a subwavelength grating waveguide was utilized for enhancing the absorption of methane on a chip.[45]

Photonics Crystal Wavegiudes and Subwavelength Grating (SWG) Waveguide. SWG waveguides consist of a periodic structure of the core, as shown in Figure 4d. The spatial period (Λ) is much smaller than the Bragg condition, that is, $\Lambda \gg \lambda/(2n_{eff})$, where λ is the light wavelength in vacuum and n_{eff} is the effective index of the waveguide. Therefore, a lossless mode is supported by SWG waveguides since the diffraction and reflection effects are suppressed. The periodic arrangement of the waveguide can be generalized also to 2D and even 3D, and utilize the slow light effect which has remarkably low group velocity.[46,47] As a result, an enhanced light-matter interaction takes place[20,34,48] and can reach even 1−2 orders of magnitude enhancement in the interaction and in the Γ factor.[19,49] It should be noted that this design has a high surface area, which may increase the surface scattering losses due to the roughness caused during the fabrication. Therefore, in the overall enhancement of the design, additional losses should be considered and not only the higher Γ.[50] The scattering losses become significant with shortening the wavelengths from mid-infrared to near-infrared for fundamental vibration spectroscopy and overtone spectroscopy, respectively.

Hollow-Core (HC) Waveguide. HC fibers and waveguides have excellent capability for guiding light in an air core with low loss over a very broad spectral range, as shown in Figure

https://doi.org/10.1021/acssensors.2c00655
ACS Sens. XXXX, XXX, XXX−XXX

4e. HC waveguides are advantageous for sensing applications as most of the field interacts with the analyte since the light is guided in a hollow geometry. This concept can be implemented in PIC platforms[51] as well as in fiber-based platforms.[52] To mitigate multimode guidance in the HC waveguide, which leads to intermodal interference, methods like antiresonant HC fiber,[53] chirped-laser dispersion spectroscopy,[54] and photothermal spectroscopy[35,55] can be used.

Microcavity Ring Resonator. Optical microcavity ring resonators enhance optical path lengths while maintaining small footprints. The sensitivity of microcavity ring resonators are related to the effective path length that light travels while circulating in the ring. As a result, the effective path length is longer than the actual path length. The effective path length L_{eff} can be determined from the quality factor Q of the ring resonance as $L_{\text{eff}} = \Gamma\frac{Q\lambda_0}{2\pi n_{\text{eff}}}$. Here λ_0 is the resonance wavelength of the microcavity and Q is the quality factor of the microcavity resonator while a typical value of Q is order of 10^5. The resolution of the microcavity device is determined by the free spectral range (FSR) between resonance wavelengths which is dependent on the ring circumference. Therefore, the compactness of these devices is at the cost of reduced resolution.[41] In opposition to a ring resonator, a straight waveguide, without a ring, would have to be tens of times longer to achieve the same orders of sensitivities.[41]

For increasing the interaction path, spatially efficient designs have been conducted, such as spiral or zigzag configurations,[36] as shown in Figure 4f. Such bent waveguide implementations enable a relatively large path in a tiny footprint, for example, a total footprint of 16 mm^2 for a 10 cm waveguide device.[36]

Table 1 compares most common materials used for on-chip overtone spectroscopy in the near-infrared. Waveguide configurations and the limit of detection (LoD) for detecting different analytes are indicated for the reported wavelengths.

WHAT COULD BE THE FUTURE APPLICATIONS OF OVERTONE SPECTROSCOPY?

Overtone spectroscopy, an analytical technique that takes advantage of high-order vibrational transitions of a molecule, can be of great significance to the scientific community in many fields, such as protein characterization, nanoscale semiconductor analysis, and space exploration, to list only a few. Since different molecules with different combinations of atoms produce unique spectra, overtone spectroscopy can be used to qualitatively identify substances but at shorter wavelengths compared to infrared spectroscopy. In addition, the intensity of the peaks in the spectrum is proportional to the amount of substance present in the sample, enabling its application for quantitative analysis.

Overtone spectroscopy can be used for medical applications due to the low absorption by tissue and water in the NIR.[33] In addition, for medical research, the sensor can be used just once for hygienic reasons, so the design should also consider the advantage of the low cost of NIR platforms.

Biomedical and gas sensing using PIC is another domain that has been widely investigated and demonstrated at the academic level, with thousands of works and dozens of reviews covering many optional configurations, platforms, and designs. However, this extensive academic work has rarely ripened into a mature industrial device.

MULTIDISCIPLINARY EXPERTISE

As with other areas, multidisciplinary expertise is certainly needed to speed up the development of overtone sensing. Here, the collaboration will likely involve at the very least researchers experienced in photonics, chemistry, engineering, clinical diagnosis, and environmental analysis. Chemists will be able to expand the palette of the surface modification to attract the probe molecules and design novel and robust methods to modify the sensors. The engineering of a novel optical setup will enable new possibilities to interrogate the optical signals. Developing miniaturized optical instruments with functions comparable to a full overtone-based spectrometer is for certain a pressing and challenging direction. The end users, whether working for biomedical or environmental purposes, will likely tell us what is urgently needed concerning the variety and concentration ranges of target substances and, more importantly, provide feedback as to whether they are satisfied with the sensor performance. We believe that with contributions from researchers with different knowledge bases and common interests, a bright future is ahead for overtone spectroscopy-based optical sensors.

CONCLUDING REMARKS

With this perspective, we aimed to point out where more effort is needed to bring overtone spectroscopy, and consequently our understanding of engineered systems, to the next on-chip level. As scientists and engineers within the community, we need to put forth effort to develop sensors for analytes that we cannot yet identify. We need to learn from neighboring disciplines in areas like mid-infrared spectroscopy and data analysis. However, most importantly, we need to reach out to other fields to find the needs and to see the possibilities that arise from and with overtone spectroscopy. Interdisciplinary approaches have the potential to reform the field and open up new avenues in chemical and biological sensing, monitoring, and diagnostics.

AUTHOR INFORMATION

Corresponding Author

Alina Karabchevsky − *School of Electrical and Computer Engineering, Ben-Gurion University of the Negev, Beer-Sheva 8410501, Israel; Isle Katz Institute for Nanoscale Science & Technology, Ben-Gurion University of the Negev, Beer-Sheva 8410501, Israel;* orcid.org/0000-0002-4338-349X; Email: alinak@bgu.ac.il

Authors

Uzziel Sheintop − *School of Electrical and Computer Engineering, Ben-Gurion University of the Negev, Beer-Sheva 8410501, Israel; Isle Katz Institute for Nanoscale Science & Technology, Ben-Gurion University of the Negev, Beer-Sheva 8410501, Israel*

Aviad Katiyi − *School of Electrical and Computer Engineering, Ben-Gurion University of the Negev, Beer-Sheva 8410501, Israel; Isle Katz Institute for Nanoscale Science & Technology, Ben-Gurion University of the Negev, Beer-Sheva 8410501, Israel;* orcid.org/0000-0002-7924-9065

Complete contact information is available at: https://pubs.acs.org/10.1021/acssensors.2c00655

Notes

The authors declare no competing financial interest.

https://doi.org/10.1021/acssensors.2c00655
ACS Sens. XXXX, XXX, XXX−XXX

■ ACKNOWLEDGMENTS

A.K. acknowledges the support of the Israel Science Foundation (ISF no. 2598/20).

■ REFERENCES

(1) Kirchhoff, P.; Bunsen, P. IX. Chemical analysis by spectrum-observations. *Philos. Mag. J. Sci.* **1860**, *20*, 88−109.
(2) Struve, W. S. *Fundamentals of Molecular Spectroscopy*; Wiley: New York, 1989.
(3) Atkins, P. W.; Friedman, R. S. *Molecular Quantum Mechanics*; Oxford University Press: Oxford, 2011.
(4) Karabchevsky, A.; Katiyi, A.; Ang, A. S.; Hazan, A. On-chip nanophotonics and future challenges. *Nanophotonics* **2020**, *9*, 3733−3753.
(5) Zhou, Z.; Yin, B.; Michel, J. On-chip light sources for silicon photonics. *Light Sci. Appl.* **2015**, *4*, e358.
(6) Grillot, F.; Duan, J.; Dong, B.; Huang, H. Uncovering recent progress in nanostructured light-emitters for information and communication technologies. *Light Sci. Appl.* **2021**, *10*, 156.
(7) Cheng, Q.; Bahadori, M.; Glick, M.; Rumley, S.; Bergman, K. Recent advances in optical technologies for data centers: a review. *Optica* **2018**, *5*, 1354−1370.
(8) Liang, Y.; Li, C.; Huang, Y.-Z.; Zhang, Q. Plasmonic Nanolasers in On-Chip Light Sources: Prospects and Challenges. *ACSnano* **2020**, *14*, 14375−14390.
(9) Cheben, P.; Halir, R.; Schmid, J. H.; Atwater, H. A.; Smith, D. R. Subwavelength integrated photonics. *Nature* **2018**, *560*, 565−572.
(10) Lin, H.; Luo, Z.; Gu, T.; Kimerling, L. C.; Wada, K.; Agarwal, A.; Hu, J. Mid-infrared integrated photonics on silicon: a perspective. *Nanophotonics* **2017**, *7*, 393−420.
(11) Michel, J.; Liu, J.; Kimerling, L. C. High-performance Ge-on-Si photodetectors. *Nat. Photonics* **2010**, *4*, 527−534.
(12) Reed, G. T.; Mashanovich, G.; Gardes, F. Y.; Thomson, D. J. Silicon optical modulators. *Nat. Photonics* **2010**, *4*, 518−526.
(13) Dai, D. Silicon Nanophotonic Integrated Devices for On-Chip Multiplexing and Switching. *Journal of Lightwave Technology* **2017**, *35*, 572−587.
(14) Karabchevsky, A.; Hazan, A.; Dubavik, A. All-Optical Polarization-Controlled Nanosensor Switch Based on Guided-Wave Surface Plasmon Resonance via Molecular Overtone Excitations in the Near-Infrared. *Advanced Optical Materials* **2020**, *8*, 2000769.
(15) Guo, J.; Dai, D. Silicon nanophotonics for on-chip light manipulation. *Chinese Physics B* **2018**, *27*, 104208.
(16) Marris-Morini, D.; Vakarin, V.; Ramirez, J. M.; Liu, Q.; Ballabio, A.; Frigerio, J.; Montesinos, M.; Alonso-Ramos, C.; Le Roux, X.; Serna, S.; Benedikovic, D.; Chrastina, D.; Vivien, L.; Isella, G. Germanium-based integrated photonics from near- to mid-infrared applications. *Nanophotonics* **2018**, *7*, 1781−1793.
(17) Wei, J.; Ren, Z.; Lee, C. Metamaterial technologies for miniaturized infrared spectroscopy: Light sources, sensors, filters, detectors, and integration. *J. Appl. Phys.* **2020**, *128*, 240901.
(18) Holler, E.; West, D.; Skoog, D. *Analytical Chemistry*; Saunders College Publishing: Philadelphia, 1994.
(19) Mortensen, N. A.; Xiao, S. Slow-light enhancement of Beer-Lambert-Bouguer absorption. *Appl. Phys. Lett.* **2007**, *90*, 141108.
(20) Lai, W.-C.; Chakravarty, S.; Wang, X.; Lin, C.; Chen, R. T. Photonic crystal slot waveguide absorption spectrometer for on-chip near-infrared spectroscopy of xylene in water. *Appl. Phys. Lett.* **2011**, *98*, 023304.
(21) Born, M.; Wolf, E. *Principles of Optics: Electromagnetic Theory of Propagation, Interference and Diffraction of Light*; Elsevier: Amsterdam, 2013.
(22) Katiyi, A.; Karabchevsky, A. Figure of merit of all-dielectric waveguide structures for absorption overtone spectroscopy. *Journal of Lightwave Technology* **2017**, *35*, 2902−2908.
(23) Dewanjee, A.; Aitchison, J. S.; Mojahedi, M. Experimental Demonstration of a High Efficiency Compact Bilayer Inverse Taper Edge Coupler for Si Photonics.*2016 IEEE Photonics Conference (IPC)*; IEEE, 2016; pp 414−415 DOI: 10.1109/IPCon.2016.7831163.
(24) Ghaffari, A.; Djavid, M.; Abrishamian, M. S. Power splitters with different output power levels based on directional coupling. *Applied optics* **2009**, *48*, 1606−1609.
(25) Yamada, H.; Chu, T.; Ishida, S.; Arakawa, Y. Optical directional coupler based on Si-wire waveguides. *IEEE Photon. Technol. Lett.* **2005**, *17*, 585−587.
(26) Lu, Z.; Yun, H.; Wang, Y.; Chen, Z.; Zhang, F.; Jaeger, N. A.; Chrostowski, L. Broadband silicon photonic directional coupler using asymmetric-waveguide based phase control. *Opt. Express* **2015**, *23*, 3795−3808.
(27) Hiraki, T.; Aihara, T.; Hasebe, K.; Takeda, K.; Fujii, T.; Kakitsuka, T.; Tsuchizawa, T.; Fukuda, H.; Matsuo, S. Heterogeneously integrated III−V/Si MOS capacitor Mach−Zehnder modulator. *Nat. Photonics* **2017**, *11*, 482−485.
(28) Li, G.; Krishnamoorthy, A. V.; Shubin, I.; Yao, J.; Luo, Y.; Thacker, H.; Zheng, X.; Raj, K.; Cunningham, J. E. Ring resonator modulators in silicon for interchip photonic links. *IEEE J. Sel. Top. Quantum Electron.* **2013**, *19*, 95−113.
(29) Epping, J. P.; Hellwig, T.; Hoekman, M.; Mateman, R.; Leinse, A.; Heideman, R. G.; van Rees, A.; van der Slot, P. J.; Lee, C. J.; Fallnich, C.; et al. On-chip visible-to-infrared supercontinuum generation with more than 495 THz spectral bandwidth. *Opt. Express* **2015**, *23*, 19596−19604.
(30) Liu, X.; Pu, M.; Zhou, B.; Krückel, C. J.; Fülöp, A.; Torres-Company, V.; Bache, M. Octave-spanning supercontinuum generation in a silicon-rich nitride waveguide. *Optics letters* **2016**, *41*, 2719−2722.
(31) Vlk, M.; Datta, A.; Alberti, S.; Yallew, H. D.; Mittal, V.; Jágerská, G. S. Extraordinary evanescent field confinement waveguide sensor for mid-infrared trace gas spectroscopy. *Light Sci. Appl.* **2021**, *10*, 26.
(32) Karabchevsky, A.; Katiyi, A.; Bin Abdul Khudus, M. I. M.; Kavokin, A. V. Tuning the Near-Infrared Absorption of Aromatic Amines on Tapered Fibers Sculptured with Gold Nanoparticles. *ACS Photonics* **2018**, *5*, 2200.
(33) Katiyi, A.; Zorea, J.; Halstuch, A.; Elkabets, M.; Karabchevsky, A. Surface roughness-induced absorption acts as an ovarian cancer cells growth sensor-monitor. *Biosens. Bioelectron.* **2020**, *161*, 112240.
(34) Lai, W.-C.; Chakravarty, S.; Zou, Y.; Chen, R. T. Multiplexed detection of xylene and trichloroethylene in water by photonic crystal absorption spectroscopy. *Opt. Lett.* **2013**, *38*, 3799−3802.
(35) Jin, W.; Cao, Y.; Yang, F.; Ho, H. L. Ultra-sensitive all-fibre photothermal spectroscopy with large dynamic range. *Nat. Commun.* **2015**, *6*, .
(36) Tombez, L.; Zhang, E. J.; Orcutt, J. S.; Kamlapurkar, S.; Green, W. M. J. Methane absorption spectroscopy on a silicon photonic chip. *Optica* **2017**, *4*, 1322−1325.
(37) Scullion, M. G.; Krauss, T. F.; Di Falco, A. Slotted Photonic Crystal Sensors. *Sensors* **2013**, *13*, 3675−3710.
(38) Pi, M.; Zheng, C.; Bi, R.; Zhao, H.; Liang, L.; Zhang, Y.; Wang, Y.; Tittel, F. K. Design of a mid-infrared suspended chalcogenide/silica-on-silicon slot-waveguide spectroscopic gas sensor with enhanced light-gas interaction effect. *Sens. Actuators, B* **2019**, *297*, 126732.
(39) Gill, P. K.; Marom, D. M. Single Mode, Air-Cladded Optical Waveguides Supported by a Nano-Fin Fabricated with Direct Laser Writing. *Appl. Sci.* **2021**, *11*, 6327.
(40) Hu, J.; Tarasov, V.; Agarwal, A.; Kimerling, L.; Carlie, N.; Petit, L.; Richardson, K. Fabrication and testing of planar chalcogenide waveguide integrated microfluidic sensor. *Opt. Express* **2007**, *15*, 2307−2314.
(41) Nitkowski, A.; Chen, L.; Lipson, M. Cavity-enhanced on-chip absorption spectroscopy using microring resonators. *Opt. Express* **2008**, *16*, 11930−11936.
(42) Grdadolnik, J. ATR-FTIR spectroscopy: Its advantage and limitations. *Acta Chim. Slov.* **2002**, *49*, 631−642.
(43) Bogaerts, W.; De Heyn, P.; Van Vaerenbergh, T.; De Vos, K.; Kumar Selvaraja, S.; Claes, T.; Dumon, P.; Bienstman, P.; Van

https://doi.org/10.1021/acssensors.2c00655
ACS Sens. XXXX, XXX, XXX−XXX

Thourhout, D.; Baets, R. Silicon microring resonators. *Laser & Photonics Reviews* **2012**, *6*, 47−73.
(44) Karabchevsky, A.; Kavokin, A. Giant absorption of light by molecular vibrations on a chip. *Sci. Rep.* **2016**, *6*, 1−7.
(45) Gervais, A.; Jean, P.; Shi, W.; LaRochelle, S. Design of slow-light subwavelength grating waveguides for enhanced on-chip methane sensing by absorption spectroscopy. *IEEE J. Sel. Top. Quantum Electron.* **2019**, *25*, 1−8.
(46) Borovkova, O.; Ignatyeva, D.; Sekatskii, S.; Karabchevsky, A.; Belotelov, V. High-Q surface electromagnetic wave resonance excitation in magnetophotonic crystals for supersensitive detection of weak light absorption in the near-infrared. *Photonics Research* **2020**, *8*, 57−64.
(47) Baba, T. Slow light in photonic crystals. *Nat. Photonics* **2008**, *2*, 465−473.
(48) Lai, W.-C.; Chakravarty, S.; Wang, X.; Lin, C.; Chen, R. T. On-chip methane sensing by near-IR absorption signatures in a photonic crystal slot waveguide. *Opt. Lett.* **2011**, *36*, 984−986.
(49) Dicaire, I.; De Rossi, A.; Combrie, S.; Thevenaz, L. Probing molecular absorption under slow-light propagation using a photonic crystal waveguide. *Opt. Lett.* **2012**, *37*, 4934−4936.
(50) Kita, D. M.; Michon, J.; Johnson, S. G.; Hu, J. Are slot and sub-wavelength grating waveguides better than strip waveguides for sensing? *Optica* **2018**, *5*, 1046−1054.
(51) Yang, W.; Ferrara, J.; Grutter, K.; Yeh, A.; Chase, C.; Yue, Y.; Willner, A. E.; Wu, M. C.; Chang-Hasnain, C. J. Low loss hollow-core waveguide on a silicon substrate. *Nanophotonics* **2012**, *1*, 23−29.
(52) Jaworski, P.; Kozioł, P.; Krzempek, K.; Wu, D.; Yu, F.; Bojęś, P.; Dudzik, G.; Liao, M.; Abramski, K.; Knight, J. Antiresonant Hollow-Core Fiber-Based Dual Gas Sensor for Detection of Methane and Carbon Dioxide in the Near- and Mid-Infrared Regions. *Sensors* **2020**, *20*, 3813.
(53) Hänsel, A.; Adamu, A. I.; Markos, C.; Feilberg, A.; Bang, O.; Heck, M. J. Integrated Ammonia Sensor Using a Telecom Photonic Integrated Circuit and a Hollow Core Fiber. *Photonics* **2020**, *7*, 93.
(54) Jaworski, P. Molecular dispersion spectroscopy in a CO2-filled all-fiber gas cells based on a hollow-core photonic crystal fiber. *Optical Engineering* **2019**, *58*, 1−8.
(55) Jaworski, P. A. Review of Antiresonant Hollow-Core Fiber-Assisted Spectroscopy of Gases. *Sensors* **2021**, *21*, 5640.
(56) Ryckeboer, E.; Bockstaele, R.; Vanslembrouck, M.; Baets, R. Glucose sensing by waveguide-based absorption spectroscopy on a silicon chip. *Biomed. Opt. Express* **2014**, *5*, 1636−1648.
(57) Charrier, J.; Brandily, M.-L.; Lhermite, H.; Michel, K.; Bureau, B.; Verger, F.; Nazabal, V. Evanescent wave optical micro-sensor based on chalcogenide glass. *Sens. Actuators, B* **2012**, *173*, 468−476.

https://doi.org/10.1021/acssensors.2c00655
ACS Sens. XXXX, XXX, XXX−XXX